# Dynamic Light Scattering

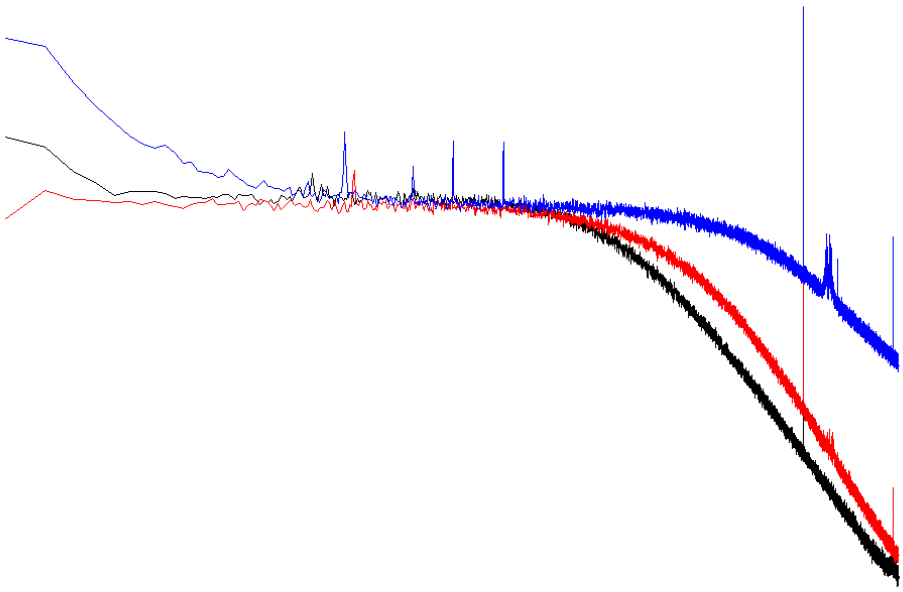

- measuring particle-size from the intensityspectrum of scattered light -

Biophysical Measurement (Physics 173) - UCSD - Spring 2002

Bernhard Englitz

Table of Contents:



List of Figures:

## 1 Introduction

Already in the 1960s it had been recognized that the innocent seeming assumption of a brownian process as the underlying process for a solution of scattering particles can be used to estimate the size of the scattering particles to an impressively high degree of accuracy [2,1]. The theoretical grounds have been worked out for both the case of isotropic and the nonisotropic scattering targets and thus the inexpensive experimental setup seems to be well suited for a whole range of measurement tasks, where homogenous solutions of particles in the range of a few to hundreds of nanometers need to be characterized.

In the present study we merely reproduce the known results for latex-spheres of known size and the protein albumine and attempt to correct our results for changes introduced by the measurement apparatus by deconvolving with the measured transfer-function.

## 2 Methods

### 2.1 Theory

The following introduction to the theory underlying this experiment is superficial in the sense that it only highlights the main ideas and assumptions, but refers the reader to the complete and very understandable treatment in the original experimental works [1,2] and the further theoretical treatises referenced therein.

Based on the assumption that particles in aqueous solution undergo diffusive motion as described by a threedimensional brownian motion, the powerspectrum of the intensity of the light scattered by this solution can be linked to the probability density function (pdf) of the brownian process, given as

$$P(r,t\,|\,0,0) = (4\pi Dt)^{-3/2}\exp(-r^2/4Dt)\,, \qquad (1)$$

Since this function only depends on D, the diffusion constant of the system, this allows to obtain a value for D, if the pdf can be measured. Luckily the diameter of the scattering particles can simply be computed from D and other known quantities via

$$D = k_B T / 6\pi\eta a\,, \quad (2).$$

This link between the pdf and the powerspectrum is a consequence of the translation of relative motion of the scattering particles into phase differences of the scattered light (see Fig.1). Thus spatial correlations are translated into phasecorrelations, which is manifested in the usage of the Wiener-Khintchine-Theorem, relating the powerspectrum to the autocorrelation of a process. Yet, phasecorrelations lead to fluctuations in the intensity of the focussed light at a detector and thus the measured quantity. Analyzing the intensity powerspectrum we can then compare the experimentally measured to the theoretically expected spectrum, namely a lorentzian line S(f) (see Eq. ).

For the following discussion it is helpful to define the "roll-off point" of the powerspectrum, which is given by the intersection of a linear (constant) fit to the low-frequency portion of S(f) and the linear fit to the high-frequency decrease (for illustration see Fig.3c). This definition is important since the quality of the fit depends mainly on how well the two fits can be tied and thus the roll-off point can be localized (also compare Fig.3a and b).

Consequently the minimally measurable diameter of the scattering particles corresponds to the roll-off point at the highest frequency which can be well defined. As we will see later this is further complicated by possibly different spectral shapes for different scattering particles as well as the noise-floor and by the transfer-function intrinsic to the measurement system.

As often in Physics theory and experimentinteract beautifully, where on the one side an extended theoretical derivation leads to a measurable prediction, which on the other hand

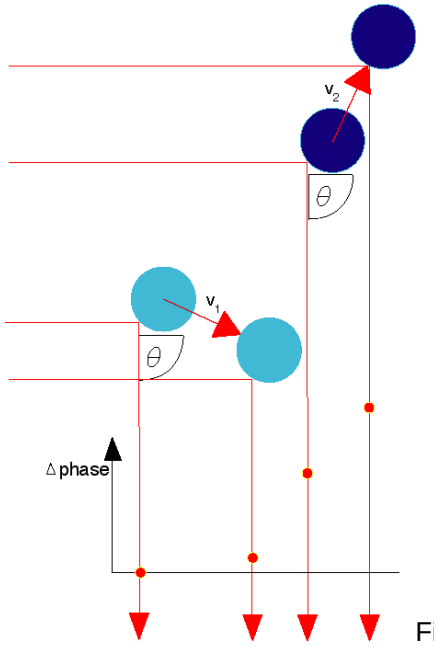


Figure 1

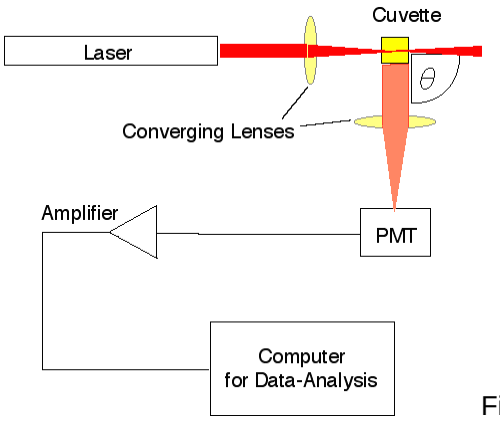


Figure 2

## 2.2 Experiment

As in almost every scattering experiment a coherent light source (HeNe Laser, l = 632nm) provides the light, which is then passed through a converging lens onto the scattering particles (Fig. 2). At a variable angle q another converging lens collects the light scattered around the q and focusses it on the collecting tube of a Photo Multiplier Tube (PMT). The PMT is powered by a powersupply, which controls the amplification of its output signal.

During different experiments, either an aperture or no aperture in front of the PMT was used, which however only amounted to scaling effects in intensity, a consequence of the obstruction of light in cases in which the aperture is present. Most experiments were conducted without an aperture, since it is hard to position the aperture directly in front of the actual tube of the PMT and still have the tube in the focal plane of the second converging lens.

For determination of the response-function of the system a light pulse (see Data Analysis for reasoning) was sent through the measurement apparatus. Using a „third hand“ a red LED was positioned in the focal plane of the converging lens in front of the PMT.

Four variables determine the amplification and filter-characteristics of the measurement apparatus, composed of the PMT and the amplifier. The following list provides the location and range of the parameters:

(i) amplifier gain g (std-value: e9), range: [e4,...,e11];
(ii) amplifier suppression, (std-value: e-7A), range: [e-10,...,e-3]A;
(iii) amplifier rise-time $t_{rise}$ (std-value: 0.01ms) [0.01,0.03,0.1,0.3,...300]ms;
(iv) PMT-Voltage Supply (std-value: 500V) [0-2500]V;

The actual parameter value for the rise-time used in the recordings are indicated in the figures, which display the results from the respective recordings. All shown recording were done at the indicated standard-values unless indicated otherwise.

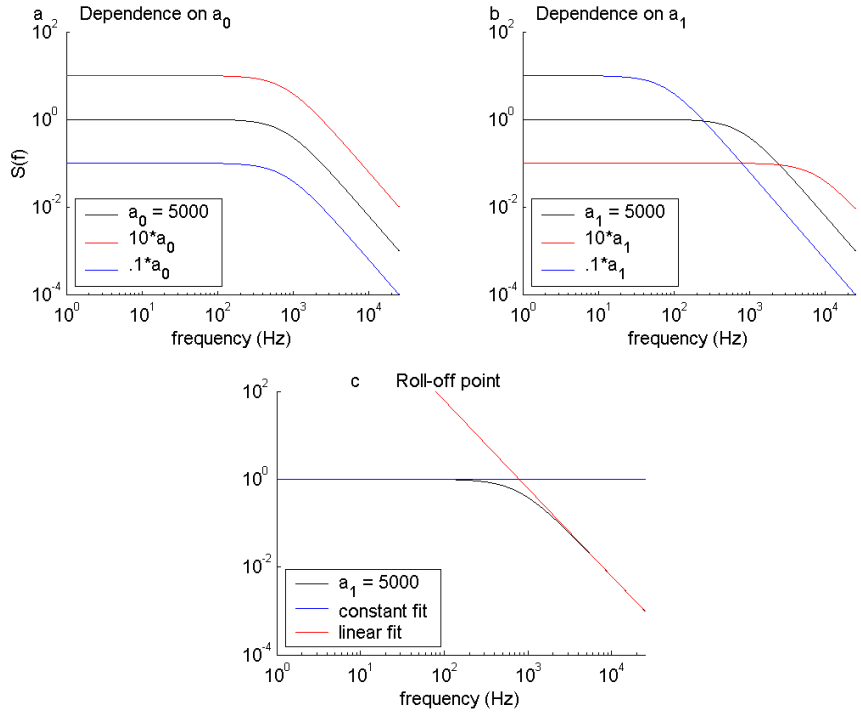


Figure 3

rinsed carefully with the solvent before the particle-containing solution was added and finally sealed with regular scotch tape. We did not find differing results if the experiment were conducted directly after or days after the preparation of the solution.

In this study we used on the one hand control media to assess control conditions: (a) distilled water (which was used to dilute the latex beads); (b) frog ringer (saline) (which was used to dissolve the albumine); (c) air, to assess the difference to water. And on the other hand several solutions were prepared : (a) latex silicon beads of three different, known sizes (500nm,50nm,20nm) and at different concentrations (50µL,100µL,400µl/mL $H_2O$) were used to calibrate the measurement system, see data-sheet at [3] for detailed information. ; (b) the protein albumine in two different concentrations (4 and 12 spatula of dried, pure albumine/10mL frog ringer).

Measurements were only reliable for reasonably high concentrations of the beads. This proved to be problematic for the highly dyed beads (especially 500nm), since their obstruction of the direct laser light and the scattered light lead to irreparable changes of the powerspectrum. The measurements depended highly on the exacly perpendicular orientation of the cuvette with respect to the laser and the PMT

The data was collected using a National Instruments NI-DAQ board, via an analog voltage-input, whose input range was [-10V,10V]. A simple data-aquisition interface wired in LabView 6.1 (National Instruments) was used to read raw data sequences (duration of 1s, recorded at 60kHz, repeated 600 times) from the NI-DAQ board, subtract the individual average and write it to binary-files, readable under Matlab (The Mathworks). Recording for 1s only was a precaution against non-stationarities in the data, which would have manifested in a frequency-range below one hertz, which were of little interest for our study.

The whole apparatus was elevated on a six tennis-balls to reduce the effects of vibrational disturbance. During recording a blackened, metal cover prevented stray light from interfering with the collection of the scattered light by covering the whole setup. A Tektronix TDS210 Oscilloscope was used to monitor voltages during data-aquiry.

## 2.3 Data-Analysis

Next the amplified Voltage datasets (see individual.vi for details) from the PMT were imported into Matlab for further processing. Powerspectra were computed by fourier-transforming each dataset, averaging the complex frequency-spectra and multiplying the result by its conjugate. The results were validated with an approximation method (psd.m, part of the signal processing toolbox) and powerspectra obtained from the standard Labview routine (PSD.vi).

Determining the radius of the scattering particles was a two step process. First the analytically derived functional form of the lorentzian line

$$S(f) = a_0 \frac{a_1}{(2\pi f)^2 + a_1^2} \quad , \quad (3)$$

with the two free parameters $a_0$ and $a_1$ was fit to the powerspectrum. In Matlab a semi-guided fitting procedure was chosen, which consisted of first finding the correct range of the two parameters and then using the non-linear minimization function fminsearch.m to minimize the euclidean distance between the data-set and the lorentzian line. The quality of the fit was accessed visually and compared with the more automated fitting procedure used in Origin 7.0. Important to notice here is that $a_0$ enters linearly, thus only performs a scaling of the function in the range, which translates to a shift in a logarithmic representation of the range (also compare to [1] Eq.3, where the powerspectrum is only proportional to the functional expression.), and does therefore not influence the shape of the function. Although $a_1$ enters nonlinearly into the function, its effect in the loglog scaled plot can approximately be described as a shift along the frequency axis, accompanied by a rather small change in the roll-off behavior (Fig. 3 illustrates the changes S(f) undergoes as $a_0$ and $a_1$ are varied separately. Joint variation is simply the composition of the individual variations). The possibility to fit the whole function is advantagous compared to the limited method used by [1], since it takes more datapoints into account than simply measuring $f_{1/2}$(the frequency, where half-maximal-height is reached) does and therefore allows to assess the quality of the fit to the experimentally measuered powerspectrum. This turned out to be of significance since e.g. the powerspectrum of the protein albumine does not follow the shape of a lorentzian line (but note, that Dubin et al. were able to get approximate size estimates for albumin and seemed to observe ).

Second, the radius was derived as a function of the fitted parameter $a_1$ and other known quantities, which then takes the form

$$K = \frac{4\pi n}{\lambda} \sin(\theta/2)$$

$$a = \frac{2 k_B T K^2}{6\pi\eta a_1} \quad , \quad (4)$$

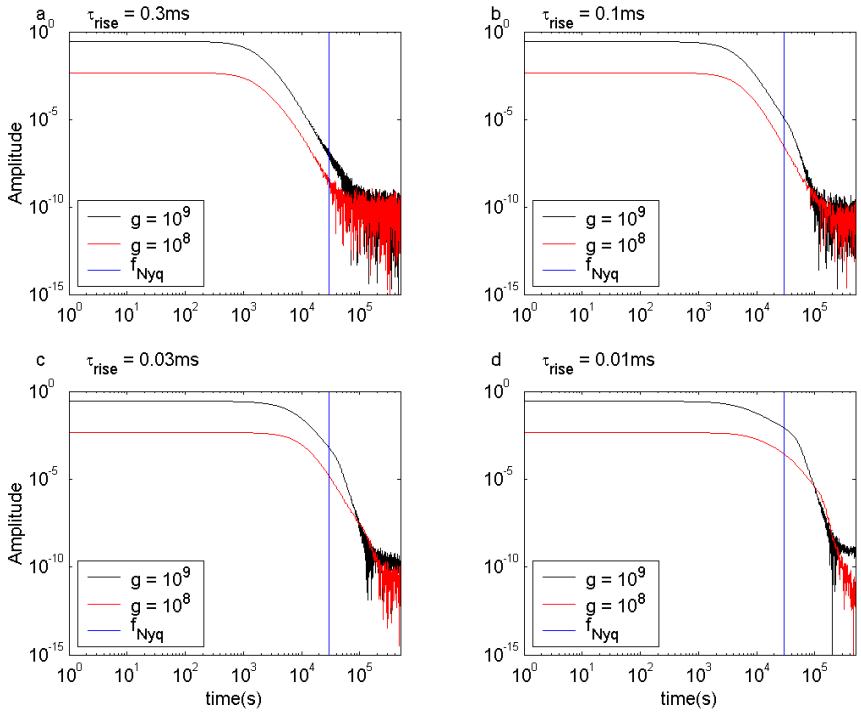


Figure 5

where T is the temperature in Kelvin (298K), $K_B$ is the Boltzman constant (1.381e-23 J/K), lambda the wavelength of the laser light (632nm), n the index of refraction of the beads (1.6 see [3], which was also used for albumine, since no other value was available), h the viscosity of the medium (1e-4 kg/sm), and q the angle of scattering (90°).

Data-processing in Origin had the caveat that the powerspectra computed by Labview have inacceptably coarse resolution for high frequencies, which due to the amplifiers filtering properties and the shape of the lorentzian line occur at very low amplitudes.

Although the recording resolution of 60kHz would have permitted to resolve the frequency spectrum up to the Nyquist limit of 30kHz, only the first 25kHz are shown due to an unidentified, strong noise-source around 26kHz, which contaminated fitting and visual display. Double logarithmic (loglog) scaling of the axes was chosen, since the shape of the lorentzian line leads to an expected inital constant part and a second exponentially decreasing part, which becomes a linear decrease in the loglog plot. These features allow quick judgement of the quality of the fit and meaningful comparison between frequencyspectra of different experimental conditions (see Fig. 3c).

Although the powerspectra resembled the general shape of a lorentzian line, the quadratic decay, dominant at higher frequencies, was for higher amplifier rise-times systematically steeper than expected. One possible reason to account for such a deviation are the frequency-filtering characteristics of the data-detection and preprocessing stage, namely the PMT and the amplifier. Assuming that these form a linear system, their characteristic impulse-response is convolved with the signal. In order to be able to reverse this operation by socalled deconvolution, the impulse-function of the system needed to be measured. We did so by feeding a very brief pulse (on the order of 50ns) of light, emitted by a red photodiode, into the system and collected the response-waveform at its output at a resolution of 1MHz. By embedding this response-waveform in a vector of one million zeros and computing its powerspectrum, we obtained the frequency-dependent amplification properties of the amplifier-PMT-circuit, which will subsequently be called the "amplifiers

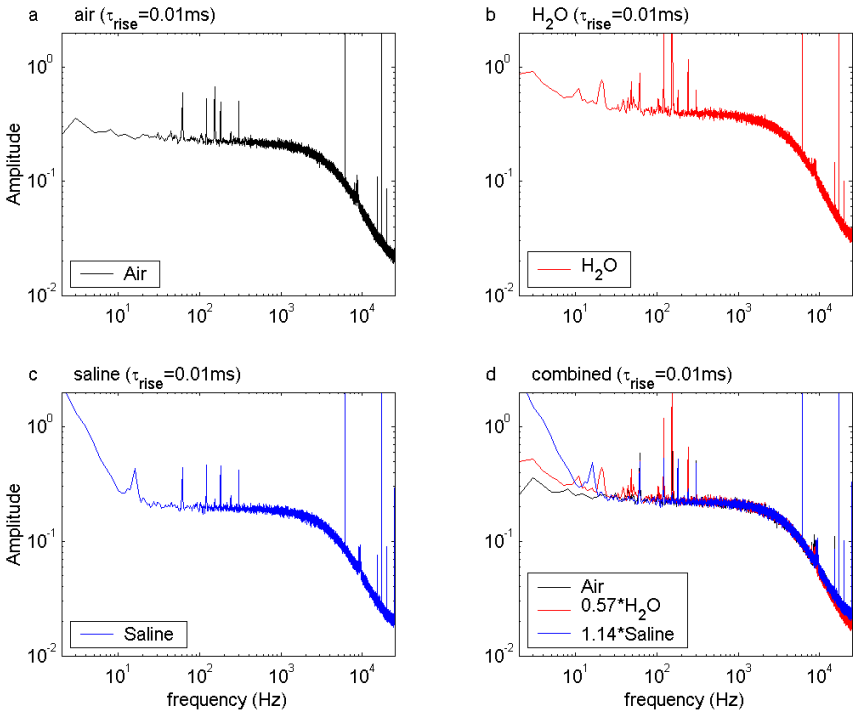


Figure 6

"amplifiers powerspectrum" makes visual comparison easier.). To then correct our measurements, namely to deconvolute, we divided the experimentally collected powerspectrum by the amplifiers powerspectrum. Thus more explicitely the amplitudes for each frequency-component are divided by the amplification amplitude for the respective frequency. Since only the shape was fitted, no normalization of the amplifiers powerspectrum was necessary. Performing this artihmetic operation directly on the powerspectra, rather than dividing the complex fouriercoefficients and then computing the powerspectrum is justified, since we are only interested in the powerspectra and $|z_1/z_2|^2 = |z_1|^2/|z_2|^2$ holds for complex-numbers $z_1$ and $z_2$.

Comparison of the impulse-responses for different settings of the rise-time and the gain, showed that it does not only have the expected dependence on the rise-time, but also a non-linear dependence on the gain, which was confirmed by comparing the shapes for different values of the gain (where the impulse-responses were scaled based on the expected gain, see Fig. 4 and 5, red and black curves). We therefore took care to only use impulse-responses for powerspectrum-corrections which were recorded at the same parameter settings.

Concerning the results presented below there often is a strong dissociation between the quality of the fit and the predictive quality of the parameter-value $a_1$ obtained from the fit. Whereas the fit often deviates substantially for higher frequencies, the lowfrequency and the roll-off region are well matched. The value obtained for $a_1$ led in all cases, i.e. different recording conditions and probes, to good predictions for the diameter of the scattering particles. We thus conjecture that despite the aberrations introduced by the measurement apparatus and possibly deviating powerspectra, the experimental setup and the data analysis procedure constitute a reliable way to estimate the diffusion constant and thus the size of the scattering particles. It should be noted that since Dubin et al. did not use a loglog plot for assessing the quality of their fit, the deviations for high frequencies might not have surfaced during their measurements.

### 3.1 Control Measurements

In order to be able to discern cuvette and solvent related from scattering particle related contributions to the powerspectrum three measurements were taken. First, distilled, filtered (Pore Size .22mu, Osmonics) water, the solvent for the beads, was measured, designated "$H_2O$" in the following and in the figures (6a). Second, filtered (Pore Size .22mu, Osmonics) frog ringer solution, the solvent for albumine was measured, designated "Saline" in the following and in the figures (6b). And third an empty cuvette was measured, which should ideally not lead to any above baseline scattering. If it contains scattering originating from the cuvette, then this forms a good controls for the two solvents. It is designated "air" in the following and in the figures (6c).

Comparison of air to both solvents shows that both solvents make a low frequency contribution, which was observed under various recording conditions (Fig. 6d). In the high frequency range on the other hand they stay remarkably close, only saline shows a small positive deviation for frequencies above 10 kHz.

Please note that the spectral shapes observed are indeed very similar to the expected lorentzian line, which could lead us to conclude that scattering particles are present. However, as can be seen in Fig. 5, the amplifiers transfer-function would lead to a fairly similar shape, characterized by the low-frequency constant region, the location of the roll-off and the linearly decreasing high-frequency region. The two shapes can be discerned by the slope of the linearly decreasing portion, which equals 2 for S(f) and greater than 2.5 for the transfer-functions. See section 3.4 for a way of correcting for the frequency dependent amplification. Although the overall amplitude level should also carry some information about the presence of scattering particles (which can directly be observed by comparing e.g. Fig. 6a and Fig. 7), this information was largely ignored, due to the imprecise reproduction of measurement conditions for different scattering probes.

### 3.2 Latex Bead Measurements

The Latex Beads constitute fairly good calibration devices, since their size and its associated standard-deviation and their index of refraction are known [3] and their shape is isotropic. Three sizes (500, 50, 20 nm) were measured.

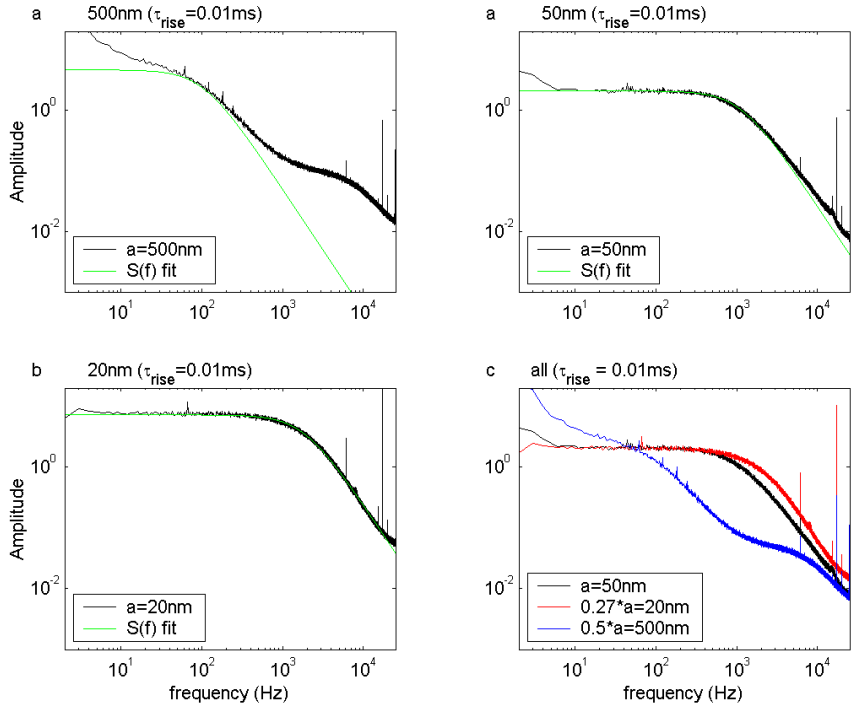


Figure 7

In the case of 500nm one can observe two deviations from the expected shape of S(f) (see Fig. 7a). The excess in low frequency amplitudes, which can be attributed to the solvent rather than the beads (see previous section) changes the powerspectrum in a way, which makes it hard to localize the roll-off point, required for fitting S(f). Further, after a region of almost linear decrease, another amplitude plateau is reached (2kHz -5 kHz), which then falls off with a slope of 2.5. Comparison with the $H_2O$ control and the transfer-function suggests, that the noise plateau is reached for these high frequencies, since the expected spectrum only contains very low amplitudes in the high frequencies. The fitting attempt shown in Fig.7a leads to a size estimate of 492nm (-1.6%), which, however, is a very unreliable fit . An alternative fit, which takes the discussed contributions into account is discussed in section 3.5.

In the case of both 50nm (Fig. 7b) and 20nm (Fig. 7c) S(f) agrees with the measured spectrum over a range of approx. 16kHz. Beyond this region both measurements start to deviate slowly in the positive direction, which is to be expected since we are approaching the noise floor of the measurement circuit. The fits lead to parameter values of $a_1$ of 7000 for the 50 nm beads and of 11500 for the 20nm beads. This corresponds to an 45.7nm (-8.6%) and 27.8 (+39%) respectively. A comparison of the different roll-off points is shown in the $a_0$-scaled powerspectra, shown in Fig. 6d.

The shown measurements for 50nm and 20nm were done at a concentration of 400µL of bead-containing solution per mL of solvent, which leads to about one percent of beads per unit volume. Lower concentrations (100µL and 50µL) did not give accurate powerspectra and are thus not shown.

Generally, the excess in low frequency amplitudes interfered with the localization of the roll-off point of the powerspectrum and thus limited measurement of larger particle sizes (>300 nm). As the particle size decreased this interference became negligible and fitting was reliable. The deduced sizes are in good agreement with the actual sizes.

## 3.3 Albumine Measurements

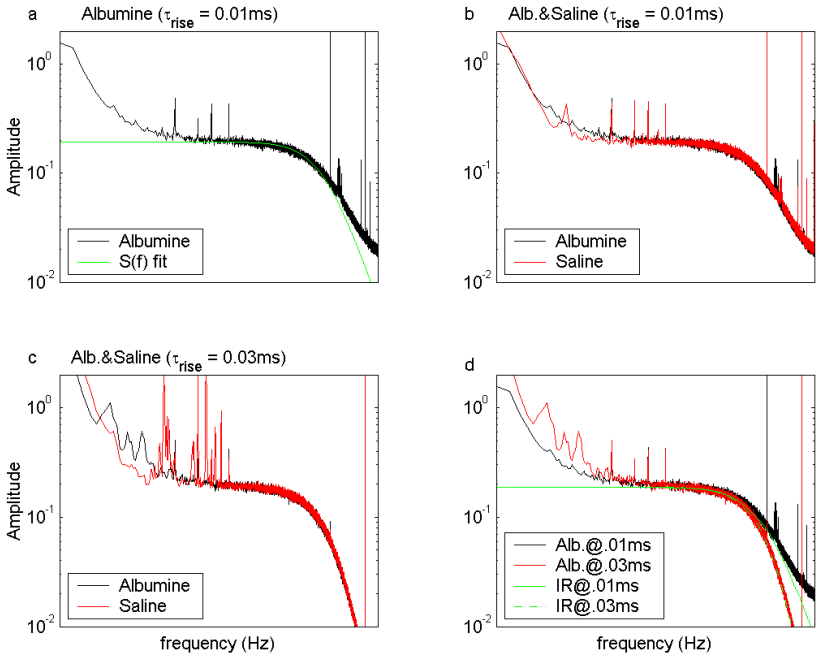


Figure 8

Encouraged by the results from the previous section, albumine, a ubiquitously occuring blood-transporter protein, which is nonisotropic and a factor of two to four smaller than the 20nm beads (5.97-9.70nm in two dimensions, PDB entry 10A6 [6]) was measured. The powerspectrum (Fig. 7a) shows a fairly clean lorentzian shape, which deviates in both the low- and the high -frequency region similar to the saline, its solvent. Fitting S(f) gives a values of $a_1$=30000, which corresponds to a diameter of 10.1nm. Although this result agrees with the expected value, a direct comparison with the powerspectrum of saline and the roll-off-properties of the transfer-function (Fig. 8b,d), reveals that this agreement is only coincidental, since albumine and saline have almost the same powerspectra and the transfer-function of the filter predicts this spectral shape for a white spectrum. This result was obtained repeatedly for two different concentrations of albumine and two different times after sample preparation. For verification the powerspectra of albumine and saline were remeasured at a slower amplifier rise-time (Fig.8c), which showed similarly close agreement. Thus we cannot draw any precise conclusions with respect to the size of albumine besides an upper limit of about 10-15nm.

A broader bandwidth of the amplifier transfer-function would overcome this problem. An alternative correction approach which makes use of the measurable amplification-properties is discussed in the next section.

### 3.4 Deconvolution Correction

As described in the Data-Analysis section, we tried to correct for the amplifiers filtering properties by deconvoluting our measured powerspectra with the measured impulse-response (see Fig. 4 and 5).

A beautiful illustration of the amplifiers cut-off bias is shown in Fig. 9a. After performing the correction, the powerspectrum for saline becomes almost flat, i.e. white, which we would expect for no scattering particles (Fig.9b). Saline measurements at a rise-time of 0.01ms are also shown to illustrate the progression for increasing frequency bandwidth (where the corrected results should theoretically have infinite bandwidth). Although we could interpret this correction to be successful, we have to point out that applying the same correction to

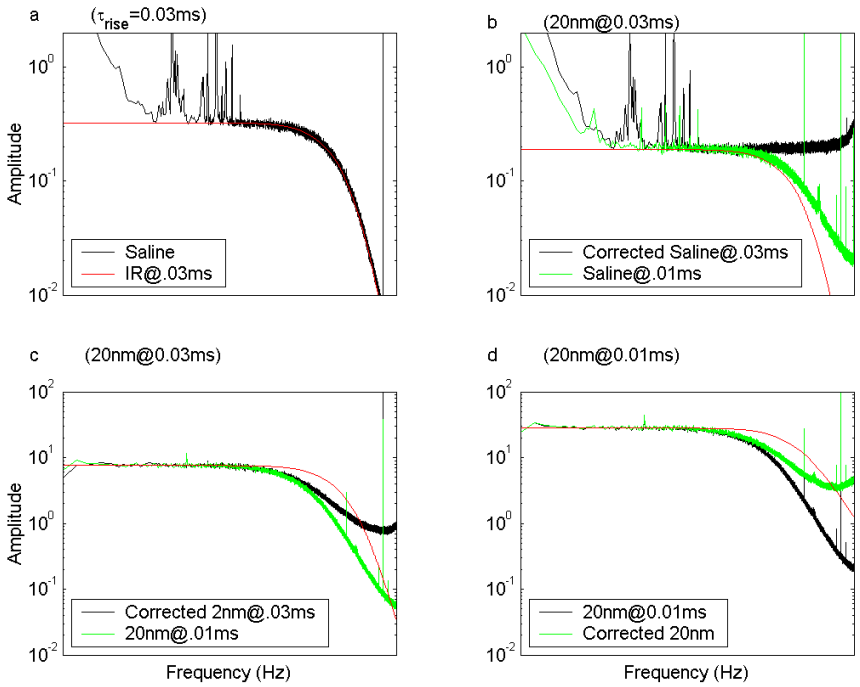


Figure 9

These corrections are shown in 8c and d for different $t_{rise}$, where the original powerspectrum can be used as a benchmark for the deviation. If we believe the correction, we would have to question, whether the powerspectrum of the beads is actually lorentzian, since the high-frequency decay is less than quadratic ($1/f^k$, where $k<2$). Yet, the final upslope of the corrected spectra can be interpreted, that we are approaching the noise-floor of the system. To take these and other deviations into account a generalized fitting function could be used which is closer to the experimental reality than the theoretical idealization, which is addressed in the next section.

### 3.5 Generalized Function for extended Fitting

In understanding experimental results by fitting theoretically derived expressions we are confined by the free parameters in the expression. To quantitatively characterize the observed deviations, we can generalize the known expression to 'explain' a greater range of phenomena. Obviously, these generalizsations remain of little explanatory value, if they cannot be tied to control results or further theoretically motivated investigation. The following generalizations take the route of using phenomena observed in control data to obtain a more flexible and better fitting expression.

The first accounts for the low-frequency contribution in both the solvents by introducing an additional additive $a_3/f^2$ term, which could be brought to close agreement with many experimental data-sets.

The second accounts for the noise-floor contribution to the measured spectra by adding a scaled version of the amplifier powerspectrum to S(f). This is based on the assumption that the initally white noise-floor is cut-off by the amplifier powerspectrum similarly to the signal. In the uncorrected case, the white noise thus takes the same shape as the amplifier powerspectrum. In the experimentally collected spectra this will only be visible if their high-frequency amplitudes decrease sufficiently fast. Thus for the 500nm case, we see an obvious contribution (Fig. 10), whereas in the other three cases it is covered by the interaction of

Initially we experimented with a third parameter, which would have changed the exponent on f in S(f) and thus yields an altered high-frequency slope in the loglog-scaled plots. However, although this parameter can account for some of the changed slopes of the powerspectra, it is not well motivated and questions the underlying theory. We found that similar corrections could be achieved by the second correction, which is more firmly grounded in the basic noise properties of the system.
The generalized Lorentzian Line S(f) can be written as follows

$$\hat{S}(f) = a_0 \frac{a_1}{(2\pi f)^2 + a_1^2} + C(f) + S_N(f), \quad C(f) = \frac{a_2}{f^2}. \qquad (5)$$

Conclusions

The estimation of the diameter of the scattering particles was possible to a good degree of accuracy for the diameters tested in this study. By comparing the results of the albumine in with the control cases and the roll-off point of the amplifier transfer-function we have to conclude, that with respect to our measuring setup, we have reached the lower bound of measuring accuracy. Obviously, this does not constitute a principal limitation, since amplifiers with a greater uniform amplification bandwidth exist.

Since size-contaminations of the latex-beads could lead to the high-frequency contributions observed for some measurements, a follow-up to this study could look at mixtures of beads and at the same time use electronmicroscopy to verify the actual size of the beads. Sums of lorentzian lines, possibly corrected for spectral deviations, would then be used to fit the experimentally observed powerspectra.

A possible future direction of this experimental method is the measurement of biological, isotropic macromolecules, e.g. Vesicles, sperical Viruses, bucky-balls etc., where the emphasis lies on isotropic, in order to guarantee a lorentzian shape of the powerspectrum. Such an approach could link functional states (e.g. docked versus released synaptic vesicles), to their characteristic powerspectra. This would, however, require an accurate estimation of the powerspectrum for fairly short stretches of data, which would consequentially not resolve the low frequency region.

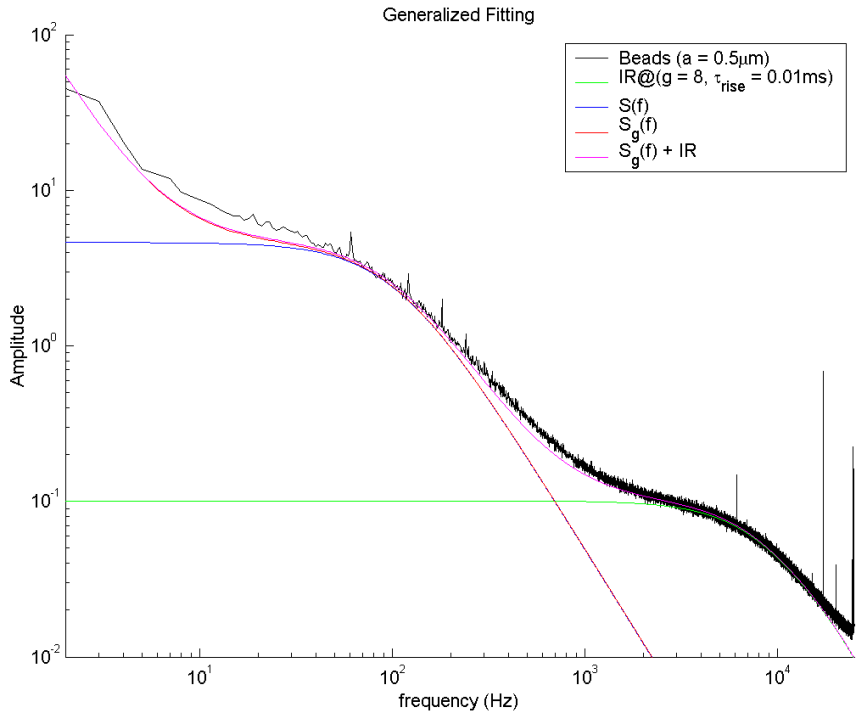


Figure 10

Alternatively, the individual shape of the powerspectrum might contain more information than just the diameter of the particle, e.g. the ratio of diameters could manifest itself in the powerspectrum. A generalized, quadratically decaying lorentzian line with additional parameters to control the low- and highfrequency behavior could then be used to extract these characteristics. Such a theory should be preceeded by a theoretically motivated hypothesis or a large-scale experimental study.

References:

[1] Clark NA, Lunacek JH, Benedek GB, A study of brownian motion using light scattering, American Journal of Physics, 38 (5), p575-585, (1970)

[2] Dubin SB, Lunacek JH, Benedek GB, Observation of the Spectrum of Light Scattered by Solutions of Biological Macromolecules, PNAS, 57(5), p1164-1171 (1967)

[3] Polysciences documentation of the Latex-spheres: www.polysciences.com

[4] Hecht E, Optics, Addison-Wesley, New York, 2001

[5] Matlab Function Index: www.mathwork.com

[6] Protein Data Bank: www.rcsb.org/pdb/

Practical Hints:

- The amplifier circuit is not ideal. Actual values of operation should always be measured rather than assumed in a calculation (e.g. Impulse response-function).
- If new beads are ordered, they should not be flourescent, since too much light get lost in the direct pass of the laser and also of the scattered light. To compensate for the second problem, the cuvette should be placed, such that the scattered laser light only has to travel a short distance before leaving the cuvette.
- Prepared cuvettes should be stored in the fridge to prevent evaporation (or have a different sealing mechanism than tape.)
- Computing the Fourier-Transform in Labview showed to be problematic in Labview, since the automatic normalization leads to a terrible resolution for the low amplitudes of the high frequencies. As a consequence the powerspectra cannot be calculated reliably for those frequencies. Besides this, data handling is easier, faster and more transparent in Matlab. Ideally one would want to circumvent LabView fully.
- Adjust the temperature control in the room to tie T.
- Use the PMT Voltage to adjust the amplification of the optical signal, rather than the Amplifier (larger bandwidth for g =8)
- If the signal fluctuates too much, try closing and opening the PMT shutter (helps sometimes)